JOURNAL OF MATERIALS SCIENCE 31 (1996) 3945–3954

Role of blend morphology in rubber-toughened polymers

R. BAGHERI, R. A. PEARSON
Department of Materials Science and Engineering, Polymer Interfaces Center, Lehigh University, Bethlehem, PA 18015, USA

The influence of blend morphology on mechanical behaviour of rubber-toughened polymers was investigated. Diglycidyl ether of bisphenol A epoxies toughnened by core–shell rubber particles were employed as the model systems. The blend morphology was varied by changing the composition of the shell of particles, the curing agent, and the extent of agitation prior to casting. It is shown that the most uniform dispersion of particles is obtained when the shell of the modifiers contains reactive groups. In the absence of the reactive groups and when a slow curing agent is employed, however, a highly connected microstructure is obtained. It was found that a blend with a connected microstructure provides significantly higher fracture toughness compared to a similar blend containing uniformly dispersed particles. The reason for this observation is that the connected morphology enables the shear bands to grow further from the crack tip and thus consume more energy before fracture occurs. Also, the yield strength in uniaxial tensile testing is significantly lower in the blend with the connected morphology. Therefore, it should contribute to a larger plastic zone size.

1. Introduction

Rubber modification, i.e. addition of a second rubbery phase, often enhances the crack growth resistance of glassy polymers without significantly compromising other desirable engineering properties. This approach was first introduced in early 1960s to overcome the inherent brittleness of some thermoplastic polymers [1] and was later employed for toughening of epoxy resins [2]. Despite the influences of volume fraction, particle size, and particle-size distribution having been significantly studied [1–5], the role of blend morphology in rubber-toughened polymers has not been thoroughly examined [6–10].

It has been shown that, depending upon the type of the polymer matrix, the type and the concentration of the elastomeric phase, the chemistry of the interface between two phases, and the processing conditions, different morphologies are obtained in rubber-modified polymers [6–10]. These morphologies can be divided into two major categories, i.e. discrete and connected microstructures. The discrete morphology contains individual particles or clusters of particles that are well separated and usually have a spherical geometry. On the other hand, the connected microstructure, also called continuous [6, 7] or inter-connected [8], contains one or several rubbery networks. There appears to be an intermediate morphology, usually at low rubber contents, in which local regions of connected particles are dispersed discretely in the matrix. Generally speaking, the aspect ratio of the second-phase particles or domains in the discrete morphology is very close to one, whereas the connected microstructure may contain very large aspect ratio particles or domains.

The consensus in the literature is that a connected morphology provides more desirable mechanical properties, especially higher toughness, compared to a discrete microstructure. However, the subject has not been critically examined. Borggreve and Gaymans [6], for example, observed a significant drop in the ductile–brittle transition (DBT) temperature in rubber-toughened nylon when the blend morphology changed from discrete to continuous. However, they could not clearly interpret their observation, because the two morphologies were obtained at different rubber contents.

Flexman *et al.* [7] argued that in rubber-modified blends, a continuous rubbery phase provides higher toughness than that of the discrete rubber particles because the former has better bridging efficiency. This idea is similar to that proposed in thermoplastic-modified epoxies [11–14] and ductile-metal-toughened ceramics [15] where the second-phase particles are potentially strong bridging elements. In rubber-toughened polymers, however, it has been shown that the rubber bridging is not a considerable toughening mechanism [4, 16]. Therefore, it is unlikely that enhanced bridging is responsible for the increase in toughness.

Yamanaka *et al.* [8] observed lower yield strength, higher damping capacity and higher peel strength in a rubber-toughened epoxy when the blend contained connected microstructure, compared to that of a blend with discrete morphology. These researchers, therefore,

0022–2461

concluded that the connected morphology results in an ease of shear yielding which may improve the fracture toughness as well [8]. Parenthetically speaking, no proper means of fracture toughness assessment was employed in their study, which weakens their argument.

Sue *et al.* [10] found a modest improvement in the fracture toughness of a DGEBA epoxy modified by core–shell rubber particles when the particles had a connected morphology compared to a well dispersed microstructure. These researchers attributed their observation to the additional toughness provided by crack deflection around the locally clustered particles. It is noteworthy that the epoxy matrix used by Sue *et al.* [10] was a highly cross-linked diglycedyl ether of bisphenol A (DGEBA)/4,4′-diamino diphenyl sulphone (DDS) resin which is not significantly toughened by rubber modification [17]. Therefore, one may expect a more pronounced influence of the morphology on fracture toughness if a more ductile epoxy is employed.

The objective of this research was therefore, to elucidate further the role of blend morphology in rubber-toughened polymers. Epoxy resins which are quite toughenable were employed as the model materials in this study. These epoxies show massive shear yielding when toughened by rubber particles and thus, the results of this study might be applicable to all polymers which are toughened via the shear yielding mechanism. Preformed core–shell rubber particles are used as toughening agents because the blend morphology can be easily varied by changing the shell chemistry without altering the composition and size of the rubbery core. The final morphology is also varied via agitation of the blend prior to casting. An explanation of the evolution of morphology in epoxies toughened by core–shell rubber particles is also given.

2. Experimental procedure

2.1. Material preparation

Two model epoxy systems were employed in this study. Both systems are based on the same diglycidyl ether of bisphenol A (DGEBA) epoxy. This is a liquid resin with epoxy equivalent weight of 187 g eq^{-1} from Dow Chemicals Co. (DER 331). Two different curing agents were employed to assist in controlling blend morphology; piperidine (PIP) and aminoethyl piperazine (AEP). The curing agents used provided different gelation times under the applied curing conditions. The gelation times observed were about 20 and 100 min for AEP- and PIP-cured materials, respectively.

Two types of commercial core–shell rubber particles were used as toughening agents in this study (Table I). The basic difference between these modifiers, as seen in Table I, is the acid functionality which exists in the shell polymer of the second modifier. The presence of acid groups in the shell material was expected to result in better dispersion of particles because the COOH groups react with epoxy and suppress the clustering of particles during the gelation process. The details of the curing schedules are as follows.

TABLE I Description of the toughening agents used

Modifier	Description of modifier
MBS	Structured core/shell latex particles comprised of a methacrylated butadiene-styrene copolymer from Rohm and Haas (PARALOID EXL-2691)
MBS–COOH	Similar to MBS plus the acid functionality in the PMMA shell (PARALOID EXL-2611)

The neat DGEBA/PIP material was made through the following steps. The epoxy resin was first heated to 80 °C in a silicone bath. Next, 5 part per hundred resin (p.h.r.) curing agent was injected slowly and mixed with epoxy for 15 min at the same temperature. Vacuum was then applied and continued stirring for another 5 min to degas the mixture. The solution was cast into a 6 mm thick aluminium mould which was preheated in a 120 °C oven. The cast material was finally cured at 120 °C for 16 h. The same curing schedule was applied to the rubber-modified resins.

Concentration of the modifier was 10 vol % in both MBS and MBS–COOH modified resins (see Table I). MBS latex particles were mixed with epoxy at 80 °C for 4 h before injecting the cross-linker. MBS–COOH particles, however, were first suspended in acetone and then the acetone was substituted by epoxy under vacuum at 80 °C. Next, particles were pre-reacted with epoxy at 140 °C for 4 h under vacuum. The suspension was cooled down to 80 °C before the curing agent was injected. This approach was found to be the best method for uniformly dispersing solid latex particles with acid functionality in epoxy matrices [18]. In order to observe the influence of the agitation on the blend morphology in DGEBA/PIP/MBS epoxy, three different mixing times, after addition of curing agent, were tried. The mixing times examined were 20, 40, and 60 min.

In the case of the DGEBA/AEP system, a stoichiometric ratio of the curing agent was mixed with epoxy at room temperature under vacuum for 10 min and then poured into a 6 mm thick aluminium mould. The cast material was allowed to gel for 1 h at room temperature and finally post-cured for 2 h at 100 °C. The same curing schedule was employed for the toughened epoxies. The concentration and method of addition of modifiers in this system were similar to those of PIP-cured system. However, the suspensions in this case were cooled to room temperature prior to addition of the curing agent. Owing to the short gelation time of the AEP-cured epoxies, the influence of the agitation on morphology of the blend was not considered in this system.

DGEBA/PIP and DGEBA/AEP epoxies were also modified by 2 vol % poly methylmethacrylate (PMMA). The PMMA pellets used have a number average molecular weight of approximately 100 000 g mol^{-1} (IRD-1 from Rohm and Haas Co). The epoxy–PMMA mixture was agitated at 160 °C and under vacuum for about 4 h until a uniform single-phase blend was obtained. Samples of the blend were cooled to room temperature and 80 °C before

addition of AEP and PIP, respectively. The remaining curing schedules were the same as those mentioned before.

2.2. Characterization techniques

The cured materials were characterized using a variety of techniques. Glass transition temperatures were determined using a differential scanning calorimetry (DSC) unit at a heating rate of 10 °C min^{-1}.

The tensile behaviour of materials was evaluated in accordance with the ASTM D638 test method. Type I dog-bone specimens (63.5 mm × 12.7 mm gauge section) were machined from the 6 mm thick plaques. The specimens were tested using a screw-driven Instron testing frame at a cross-head speed of 5 mm min^{-1}. A clip-on extensometer was used to measure strain in the specimen gauge length. The results reported are averages of three tests.

Plane strain fracture toughness, K_{IC}, was determined using single-edge-notch (SEN) specimens tested in three-point-bending (3PB) geometry (Fig. 1). The ASTM D5045 guideline was followed to measure K_{IC}. Pre-cracks were introduced to the 6 mm thick notched bars by hammering a razor blade which was chilled in liquid nitrogen. These tests were performed using a screw-driven Instron testing frame at a crosshead speed of 1 mm min^{-1}. The K_{IC} values reported represent averages of a minimum of five tests.

Fracture surfaces of the SEN-3PB specimens were examined using a Jeol 6300F scanning electron microscope (SEM) at an accelerating voltage of 5 kV. Samples were coated with a thin layer of gold–palladium before examination to protect the fracture surfaces from beam damage and also to prevent charge build up.

In order to observe the crack-tip damage zone of modified epoxies, the double-notched four-point bending (DN-4PB) method in conjunction with transmission optical microscopy (TOM) was employed [19]. Details of this technique are as follows.

First, two edge cracks of equal length were introduced into a bending sample (Fig. 2). The specimen was then loaded in a four-point bending fixture until damage zones formed at the crack tips. Finally, one of the cracks reached the instability point and propagated, causing the sample to fracture. The other crack, which was unloaded, contained a well developed damage zone that represents the conditions

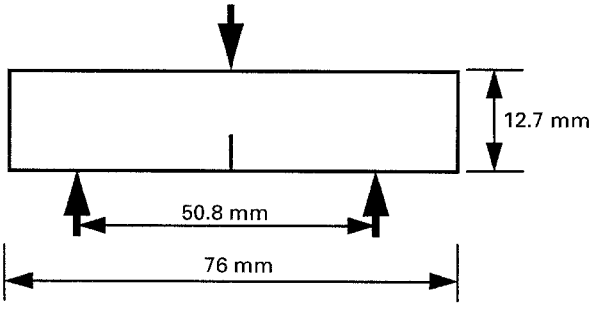

Figure 1 Schematic diagram of the SEN-3PB specimens used for fracture toughness testing.

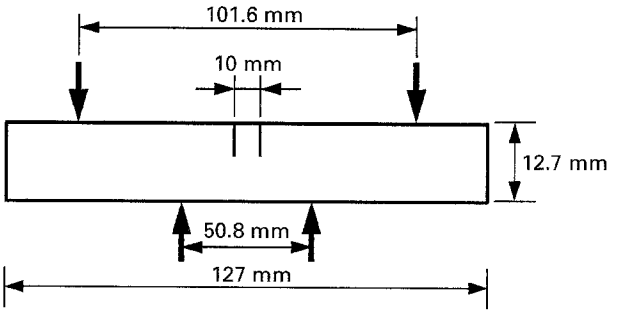

Figure 2 Schematic diagram of the DN-4PB specimens used for observation of the crack tip damage zones.

prior to the failure of the material. This damage zone could be observed using a transmission optical microscope after thinning via petrographic polishing [19]. Specimens 6 mm thick were used for this study. A screw-driven Instron testing frame at a crosshead speed of 1 mm min^{-1} was employed for breaking the samples. Thin specimens (30–50 μm) taken from the mid-plane of samples (plane strain region) were then viewed using an Olympus BH-2 transmission-light microscope.

Dynamic mechanical analyses (DMA) of PMMA-modified epoxies were performed using a Rheometrics RDA-2. A frequency of 6.28 rad s^{-1} ($\sim$1 Hz) and a strain level of 0.1%–0.3% were applied. Test specimens had dimensions of 30 mm × 10 mm × 3 mm. The temperature range of 30–150 °C was scanned in two steps with a heating rate of 5 °C min^{-1} up to 70 °C and 2 °C min^{-1} from 70–150 °C.

3. Results and discussion

The DSC analyses revealed glass transition temperatures of 87 ± 2 and 105 ± 1 °C for PIP and AEP-cured epoxies, respectively. Observation of similar glass transition temperatures for similar blends illustrates that the chemical structure of the epoxy matrix was not influenced by rubber modification in both systems. This result is particularly important in cases where epoxies are toughened by MBS–COOH particles. Note that these particles, as mentioned before, are dispersed in epoxy resins through a process of acetone–epoxy exchange. The absence of a drop in T_g indicates complete extraction of the solvent.

3.1. Blend morphology

The morphology of the blends was investigated using scanning electron microscopy (SEM) of fracture surfaces. Fig. 3 shows scanning electron micrographs taken from the stress-whitened zone of DGEBA/PIP epoxies toughened by 10 vol % MBS and MBS–COOH particles. As seen in this figure, MBS–COOH particles result in a uniform dispersion. MBS particles, however, are highly aggregated and have formed a type of continuous morphology. Therefore, Fig. 3 illustrates the strong influence of the shell composition on the blend morphology. This finding is similar to that of Sue *et al.* [10] and indicates that the blend morphology in rubber-toughened epoxies can be tailored through the chemistry of the particle/matrix interface.

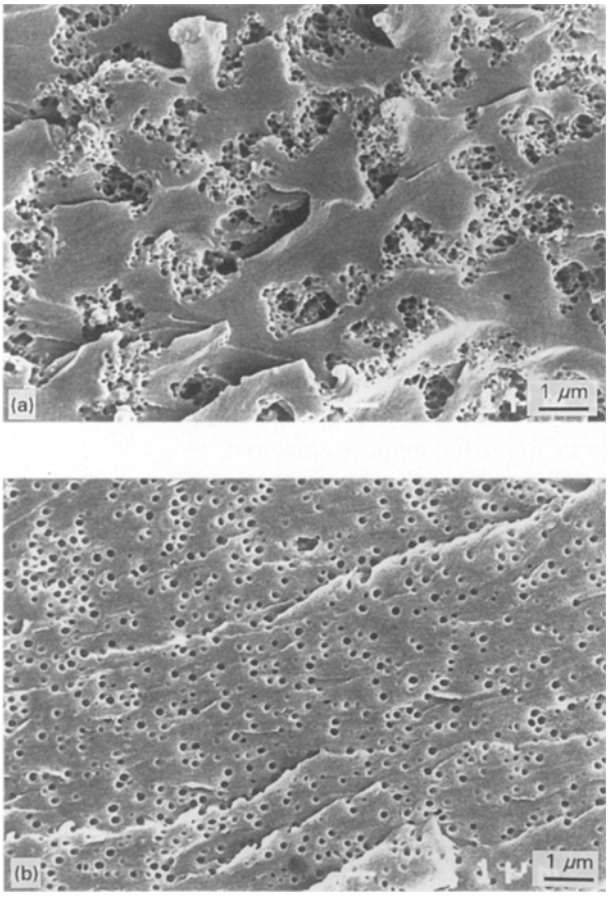

Figure 3 Scanning electron micrographs taken from the stress-whitened zone of DGEBA/PIP epoxies which are modified by 10 vol % (a) MBS and (b) MBS–COOH particles. As seen in these figures, MBS particles are aggregated, while MBS–COOH particles are uniformly dispersed. This observation illustrates the significance of shell chemistry on the blend morphology.

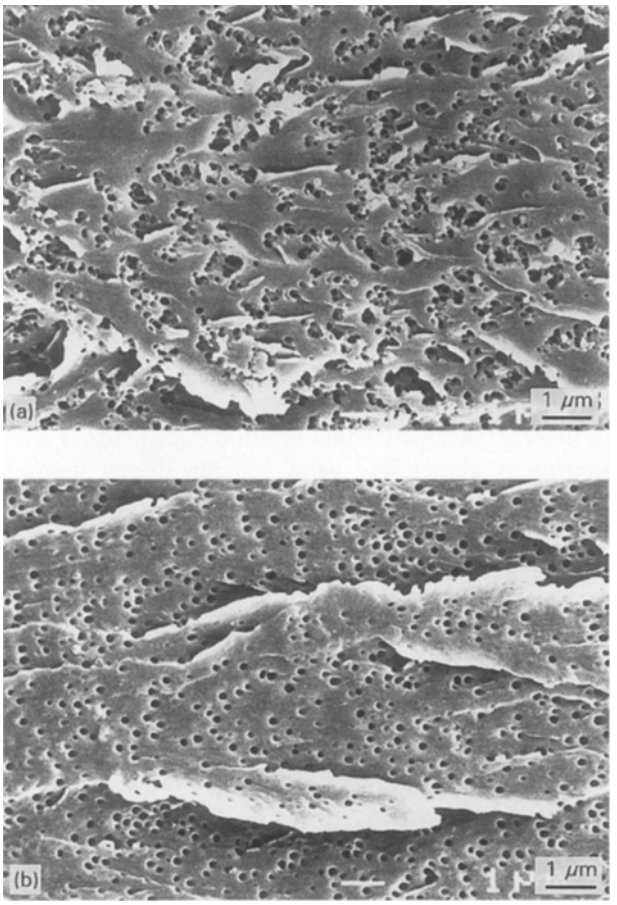

Figure 4 Scanning electron micrographs taken from the stress-whitened zone of DGEBA/AEP epoxies which are modified by 10 vol % (a) MBS and (b) MBS–COOH particles. Better dispersion of MBS particles than that of Fig. 3a illustrates the influence of curing agent in the formation of the morphology.

Scanning electron micrographs taken from the stress-whitened zone of DGEBA/AEP epoxies toughened by 10 vol % MBS and MBS–COOH particles are shown in Fig. 4. As seen in this figure, similar to that of PIP-cured epoxy, MBS–COOH particles are uniformly dispersed (Fig. 4b). MBS particles, however, have significantly different dispersion in this epoxy matrix compared to that of PIP-cured material (compare Figs 3a and 4a). MBS particles are much less aggregated in the AEP-cured epoxy compared to that of the PIP-cured material, although they still do not have the uniform dispersion of the MBS–COOH particles (Fig. 4b).

Comparing Figs 3 and 4, one concludes that not only the shell chemistry, but the type of cross-linker affects the blend morphology. Because the two epoxy systems used in this study have very different gelation times (20 and 100 min for AEP- and PIP-cured epoxies, respectively), one may attribute the influence of the cross-linker on blend morphology to the kinetics of gelation. In other words, MBS particles form the particular connected morphology seen in Fig. 3a because they have enough time for aggregation in PIP-cured matrix. In AEP-cured resin, however, particles cannot form that morphology owing to the short gelation time. Use of MBS–COOH rubber results in a uniformly dispersed morphology because the reactive groups chemically bond to the matrix and suppress clustering of particles.

This hypothesis leads to the conclusion that further agitation of the DGEBA/PIP/MBS blend should result in more uniform dispersion of particles, because it suppresses the aggregation of particles. In order to investigate the accuracy of this hypothesis, different mixing times were examined for the PIP-cured epoxy. The resulting morphologies are shown in Fig. 5. This figure shows scanning electron micrographs taken from the stress-whitened zone of the blends which were mixed for 40 and 60 min after addition of the curing agent. Notice that the micrograph shown in Fig. 3a is taken from a blend which was mixed for just 20 min after addition of the cross-linker.

In spite of no attempts to quantify the dispersion of MBS particles, comparing Figs 3a, 5a, and b, reveals that increasing the mixing time has reduced the connectivity of particles. In other words, increasing the mixing time has resulted in the formation of many isolated clusters of particles (Fig. 5), as opposed to the type of continuous morphology of rubber particles found at short mixing time (Fig. 3a). Therefore, we may conclude that the core–shell rubber particles are uniformly dispersed in epoxy resin prior to the addition of the curing agent. The curing reaction, then, provides the driving force for aggregation of particles

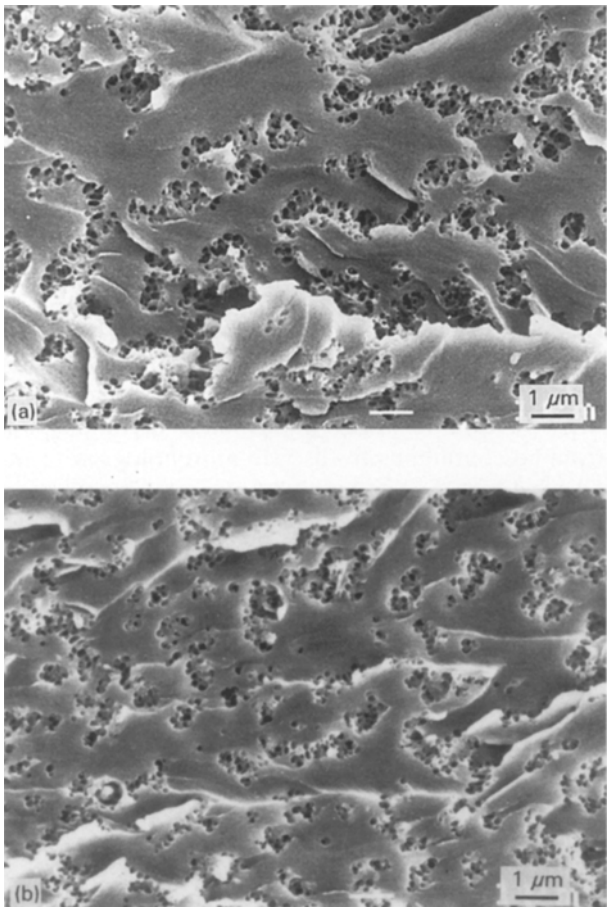

Figure 5 Scanning electron micrographs taken from the stress-whitened zone of DGEBA/PIP epoxies which are modified by 10 vol % MBS. The difference between these materials and that shown in Fig. 3a is that the mixing time which was 20 min in Fig. 3a is increased to (a) 40 min and (b) 60 min. Comparing these figures with Fig. 3a, one appreciates that increasing the mixing time has reduced the degree of connectivity of particles.

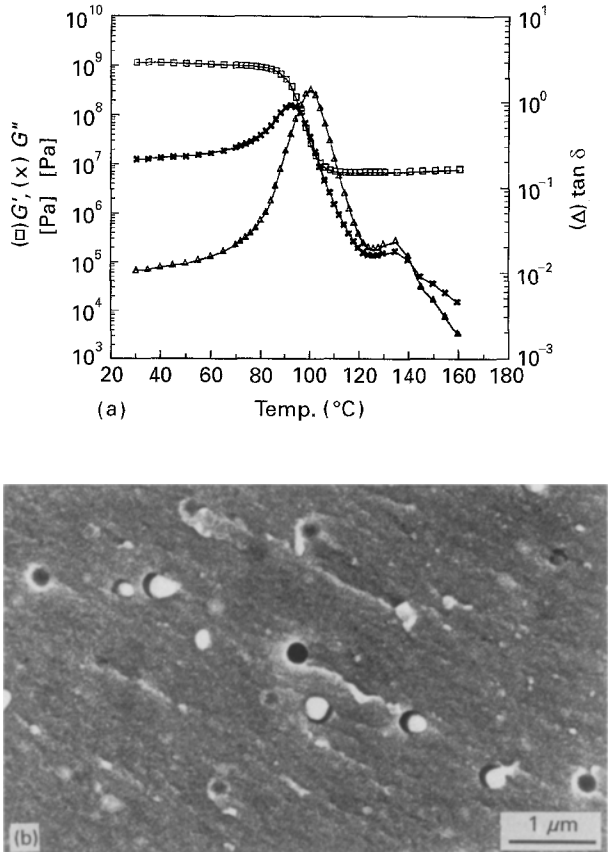

Figure 6 (a) DMA spectrum and (b) scanning electron micrograph of DGEBA/PIP epoxy modified by 2 vol % PMMA.

which may result in the formation of a highly connected morphology, as seen in Fig. 3a, in the absence of reactive groups and with a minimal agitation of the blend. This conclusion will be further proved by investigating the origin of the morphologies found in Figs 3–5.

The origin of the morphologies of MBS-modified epoxies was studied by investigating the phase separation of PMMA in epoxy matrices used. Note that the shell material of the rubber modifiers used is basically comprised of PMMA (Table I) and thus, the PMMA–epoxy interactions may provide the driving force for the formation of different morphologies in this study. For this purpose, both DGEBA/PIP and DGEBA/AEP epoxies were blended with 2 vol % PMMA. This concentration was selected because the amount of PMMA in an epoxy blend containing 10 vol % modifier is around 2 vol % [20]. The cured epoxy/PMMA blends were subjected to dynamic mechanical analysis (DMA) and scanning electron microscopy (SEM). The results of these experiments are shown in Figs 6 and 7.

The DMA spectrum of PIP-cured epoxy (Fig. 6a) shows two peaks in which the larger one belongs to the matrix and the smaller one is that of the PMMA. This observation indicates the presence of a second phase, i.e. PMMA precipitates. This conclusion is also evinced in Figure 6b which shows the second-phase particles in the scanning electron micrograph of this material.

In the case of AEP-cured epoxy, the DMA spectrum did not show two peaks (Fig. 7a). However, the scanning electron micrograph of this material indicated the presence of the second-phase particles (Fig. 7b). The reason why the DMA spectrum did not show two peaks in this case is that the DGEBA/AEP resin has a glass transition temperature (T_g) very close to that of PMMA. Therefore, the PMMA peak is almost completely hidden behind the matrix peak. Note that the DMA spectra seen in Figs 6 and 7 illustrate about 20–30 °C higher glass transition temperatures for the epoxy blends than that found using the DSC analyses. This is also the case for the PMMA peak seen in Fig. 6a. The reason for this observation is the particular testing conditions applied in the DMA test, and it does not affect the generality of the results.

The results of this study illustrate that PMMA is not miscible once either of the matrices is cured. On the other hand, Gomez and Bucknall [21] have shown that in the absence of the curing agent, PMMA is completely miscible in DGEBA epoxy. We also observed a clear single-phase epoxy–PMMA blend prior to addition of the curing agents, which indicates the miscibility of PMMA in DGEBA resin. Therefore, it is concluded that PMMA, which is originally miscible in DGEBA epoxy, precipitates out after addition of the

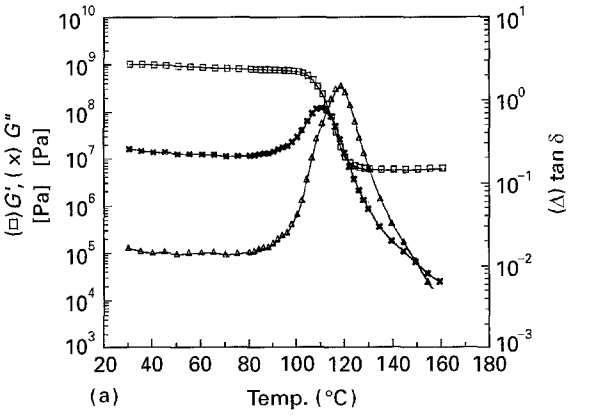

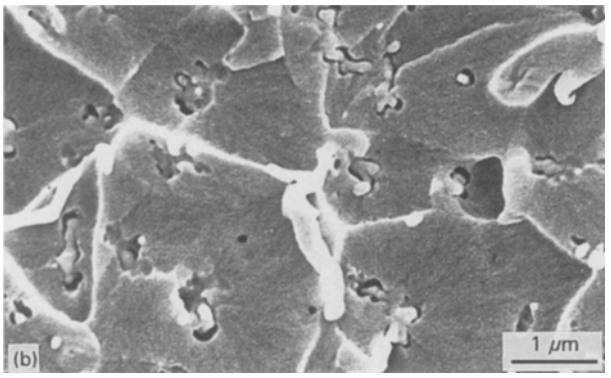

Figure 7 (a) DMA spectrum and (b) scanning electron micrograph of DGEBA/AEP epoxy modified by 2 vol % PMMA.

curing agent when the cross-linking proceeds. Consequently, we may explain the aggregation of MBS particles in epoxy based on the PMMA–epoxy interactions and through the following model.

The core–shell rubber particles are well dispersed in epoxy prior to addition of the curing agent due to the miscibility of the shell material, PMMA, with the DGEBA epoxy. As the curing reaction proceeds, the shell polymer becomes immiscible in the epoxy, and thus the uniform dispersion of the particles is thermodynamically unstable. The particles then cluster to reduce the interaction between the shell polymer and the matrix. Therefore, the final morphology of the blend is determined by a kinetic competition between the phase separation and the curing reaction. Thus, a slow curing system, like DGEBA/PIP, results in a relatively coarse segregation (Fig. 3a), whereas a fast curing system, like DGEBA/AEP, yields a more uniform morphology (Fig. 4a). Application of reactive groups, such as COOH, provides the most uniform dispersion (Fig. 3b and 4b), because epoxy-based copolymers are formed which reduce the thermodynamic driving force for precipitation. Mechanical agitation of the blend during the curing reaction also disrupts the enlargement of the connected structure (Fig. 5).

The question remains as to why, after addition of the curing agent, MBS particles tend to form the inter-connected structure seen in Fig. 3a and do not simply aggregate to discrete clusters. While the exact answer to this question is not known, two possible reasons could be proposed. Firstly, formation of this particular morphology, which is a kind of co-continuous structure [8], can be attibuted to the nature of phase separation in PMMA–epoxy blend, i.e. spinodal decomposition [21]. Notice that the co-continuous structure is very well known as a sign of spinodal decomposition in polymer blends [22]. In other words, one may simply attribute the formation of the inter-connected structure in DGEBA/PIP/MBS blend to the spinodal decomposition in the DGEBA/PIP/PMMA system. This proposal leads to the conclusion that one might be able even to obtain a discrete morphology in DGEBA/MBS blend if an extremely long gelation time is provided. The reason is the structural changes in spinodal decomposition from co-continuous to discrete morphology with increasing time. Such a hypothesis was not examined in this study.

Another approach to explain the formation of the inter-connected morphology (Fig. 3a) is to draw an analogy of the means of aggregation in colloidal suspensions. Carpineti and Giglio [23] reported that aggregation in three-dimensional colloidal suspensions of rather high volume fractions exhibits features similar to systems undergoing spinodal decomposition. This subject was further investigated by Robinson and Earnshaw [24] who spread polystyrene latex spheres on the surface of an aqueous subphase with a monolayer area fraction of about 10%. Then, they added $CaCl_2$ salt to the subphase and induced irreversible aggregation, which proceeded to gelation after several hours. Digitized images taken from different stages of this experiment showed features very similar to the morphology seen in Fig. 3a in this study. Robinson and Earnshaw [23] measured the fractal dimensions in this process and found that they corresponded to the values obtained in simulations of diffusion-limited cluster aggregation (DLCA) in two dimensions. Therefore, one may also explain the formation of the inter-connected structure in MBS-toughened epoxy by means of DLCA process.

3.2. Mechanical characterization

The results of the mechanical characterizations performed on both PIP and AEP-cured epoxies are shown in Table II. As seen in this table, the neat epoxies used in this study have similar mechanical properties. Resins containing MBS–COOH particles also show similar mechanical performance. The response of these epoxy resins to MBS particles, however, is very different. Table II also illustrates that while application of MBS and MBS–COOH modifiers result in very different mechanical properties in PIP-cured resin, they provide nearly equivalent properties in AEP-cured material.

Comparing the results of mechanical characterizations (Table II) with those of the blend morphologies (Figs 3 and 4), one appreciates the significance of blend morphology on the mechanical behaviour of the blend. Notice that in PIP-cured epoxies, where application of MBS and MBS–COOH particles resulted in very different morphologies (Fig. 3), mechanical properties of blends also varied significantly (Table II).

TABLE II Mechanical characterization of neat and rubber-modified blends

System	Modifier[a]	Young's modulus[b] (GPa)	Yield stress[b] (MPa)	Fracture toughness[c] (MPa m$^{0.5}$)
PIP-cured				
	None	2.80	71	0.90
	MBS	2.50	54	2.80
	MBS–COOH	2.50	65	2.15
AEP-cured				
	None	2.75	75	0.85
	MBS	2.50	61	2.25
	MBS–COOH	2.50	63	2.15

[a] Modifier content for rubber-toughened epoxies is 10 vol %.
[b] Young's modulus and yield stress were measured in tensile test.
[c] Fracture toughness values were determined using single-edge notched specimens tested in three-point bending.

On the other hand, in AEP-cured resins where the application of two modifiers did not yield very different microstructures (Fig. 4), mechanical properties were also nearly equivalent (Table II). Being more specific, the particular morphology formed in DGEBA/PIP/MBS blend (Fig. 3a), resulted in a superior fracture toughness (Table II). This morphology, however, resulted in a lower yield stress compared to the uniformly dispersed microstructure (Table II). Our other study [18] revealed that the blends with discrete and connected morphologies have equivalent yield stresses when they contain 15 and 10 vol % rubber, respectively.

Because the connectivity of the rubber particles is the major characteristic of the morphology seen in Fig. 3a, it could be claimed that a connected structure of particles results in improved toughness compared to that of a uniformly dispersed morphology. This claim is further supported by the results shown in Table III which illustrate the fracture toughness of MBS-modified epoxies as a function of mixing time in DGEBA/PIP matrix. Notice that increasing the mixing time reduced the degree of connectivity among the particles (Figs 3a, 5a and b) and correspondingly, the fracture toughness of the blends (Table III).

Similar to our tensile results, Yamanaka *et al.* [8] found that a rubber-toughened blend with the connected morphology reveals a lower yield stress than a blend containing the discrete morphology. Based on this observation, Yamanaka *et al.* [8] expected that the blend with the connected morphology would exhibit a higher fracture toughness. In spite of the results of our present study, i.e. the blend with lower yield stress has higher fracture toughness, we believe that one cannot make a direct correlation between the uniaxial tensile testing and the fracture toughness test results. The reason is that the stress states in the two test methods are significantly different and also the tensile test represents the global properties of the material, while the fracture toughness is the local response of the material at the crack tip. In other words, reducing the yield stress does not necessarily result in improved fracture toughness. This claim is further supported by the reduction seen in both yield stress and fracture toughness of rubber-modified epoxies when the micrometre or sub-micrometre size particles are replaced by 40 [18] or 150 μm size particles [4].

The superiority of the connected structure in improving the fracture toughness of rubber-toughened epoxy found in this investigation contradicts the analytical study of Huang [25]. These researchers claimed that for a given particle size, the fracture toughness of a rubber-modified blend depends on both concentration and dispersion of the particles. Huang [25] showed in their model that the maximum toughness is obtained at low rubber concentration in a blend containing uniformly dispersed particles. In a blend with connected morphology, however, the maximum toughness is obtained at rather higher modifier contents [25]. Having this in mind, one may claim that we could have obtained higher fracture toughness in blends with uniform structure, if we employed less than 10 vol % rubber. This claim is simply refuted by our own results [18] which shows the maximum toughness in a rubber-modified epoxy with uniform dispersion of particles is obtained at 10 vol % modifier.

TABLE III Effect of mixing time[a] on the fracture toughness in DGEBA/PIP epoxy toughened by 10 vol % MBS rubber

Mixing time (min)	Fracture toughness (MPa m$^{0.5}$)	Comments
20	2.80	Morphology seen in Fig. 3a
40	2.55	Morphology seen in Fig. 5a
60	2.40	Morphology seen in Fig. 5b

[a] The time period between injection of the curing agent and casting of the blend into the mould.

3.3. Toughening mechanism

The results of this study provide evidence that a connected morphology is superior to a discrete microstructure in improving the fracture toughness of a rubber-modified epoxy. It is now necessary to elucidate the mechanism responsible for this difference in crack growth resistance.

It was mentioned before that rubber bridging [7] and crack deflection [10] have been proposed as possible reasons for the superior fracture toughness of

TABLE IV Plastic zone sizes in DGEBA/PIP system

Modifier	Observed plastic zone size[a] (μm)	Predicted plastic zone size[b] (μm)	Normalized plastic zone size[c]
MBS	800	285	2.81
MBS–COOH	250	116	2.15

[a] Maximum width measured in Fig. 8.
[b] Plane strain plastic zone size ($2r_y$ in Equation 1).
[c] Observed divided by predicted plastic zone size.

a blend with connected morphology. In this study, crack tip damage zone of two PIP-cured materials were examined using transmission optical microscopy (TOM) to investigate the mechanism responsible for the enhanced toughness of the inter-connected structure.

Fig. 8a and b represent the transmission optical micrographs taken from the crack tip damage zone of MBS and MBS–COOH modified materials, respectively. These figures correspond to the materials of which their morphology is shown in Fig. 3a and b, respectively. As seen in Fig. 8, the MBS-modified material has a significantly larger plastic zone size than the MBS–COOH modified epoxy. Therefore, it may be concluded that the enlargement of the crack tip plastic zone is the origin of extra toughness in MBS-modified epoxy. On the other hand, because the two blends have different yield stresses (Table II), different plastic zone sizes are anticipated [26]. Consequently, one needs to take into account the effect of yield stress on the crack tip plasticity. This can be done through normalizing the plastic zone size by the yield stress of the blend.

Table IV compares the sizes of observed plastic zone, expected plastic zone, and normalized plastic zone of epoxies toughened by MBS and MBS–COOH modifiers. The observed plastic zone size is obtained by measuring the maximum width of the damage zones seen in Fig. 8. The expected size is calculated as $2r_y$ in the Irwin equation (Equation 1) for the plane strain plastic zone size [26]. The normalized value is then the ratio of the observed versus the predicted plastic zone size.

$$r_y = \frac{1}{6\pi}\frac{K_{IC}^2}{\sigma_{YS}^2} \quad (1)$$

where r_y is the radius of the plain strain plastic zone size, K_{IC} the plain strain fracture toughness, and σ_{YS} the yield stress in tension.

Interestingly, as seen in Table IV, the normalized plastic zone size is significantly larger for the MBS-modified epoxy, which means that the increase in crack tip plasticity cannot be attributed to the reduction in yield stress alone. Therefore, one may hypothesize that shear bands can further grow at the crack tip and form a larger plastic zone size when the rubber particles possess a connected morphology compared to when the particles are uniformly dispersed.

In addition to the difference in the plastic zone size, Fig. 8 illustrates a difference in the nature of the boundary of the plastic zone in two materials. As seen in this figure, the plastic zone in MBS-modified material has a diffuse boundary, whereas a sharp boundary is observed in the case of MBS–COOH toughened epoxy. This is also an indication of the ease of shear-band propagation in MBS-modified epoxy. Therefore, the results of this study illustrate that shear bands can grow further at the crack tip and result in larger plastic zone size and higher fracture toughness, when the blend contains connected morphology. On the other hand, the shear-band propagation will be limited in blend with the discrete microstructure which results in smaller plastic zone size and lower fracture toughness. In such a case, shear-band growth is uniformly suppressed at the plastic/elastic interface.

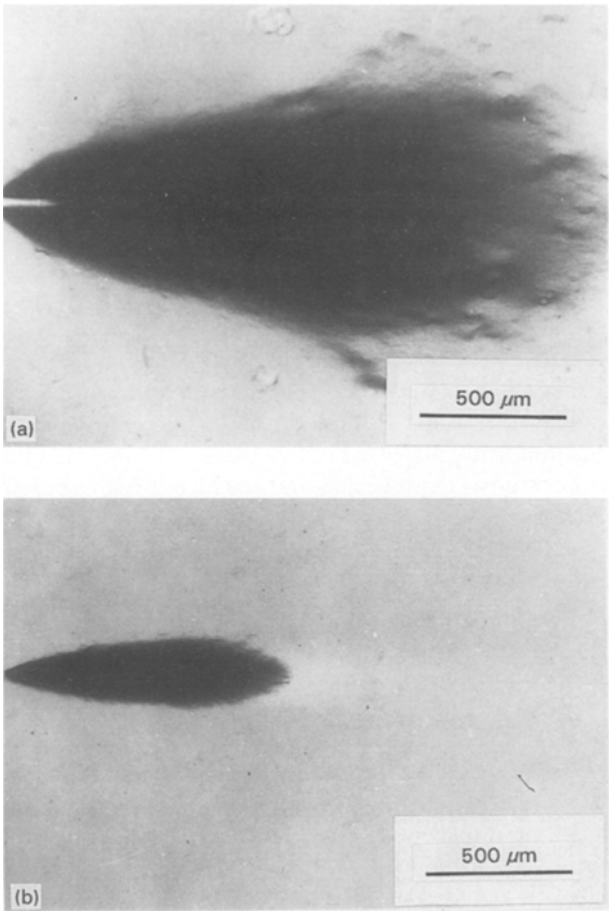

10 vol % (a) MBS and (b) MBS–COOH particles. The plastic zone observed in (a) not only is much larger, but also has a diffuse boundary compared to that of the MBS–COOH modified resin (b). This observation indicates that shear bands propagate more easily when the particles possess a connected microstructure.

This finding refutes the idea of rubber bridging [7] and crack deflection [10] being the origin of the superior toughness in blends with the connected microstructure. However, it is consistent with the prediction of Wu [27], who believed that fluctuations that result in the formation of inter-connected structure or asymmetrical morphology are in favour of fracture toughness in rubber-modified polymers. Wu [27] claimed that the rubber networks or ribbons provide a lower percolation threshold compared to that of the discrete rubber particles, which facilitates shear yielding/crazing in polymer matrices. Wu's analysis [27] did not attempt to predict the plastic zone sizes at crack tips.

One should note that our interpretation regarding the influence of blend morphology on the extent of shear-band propagation is different from the idea of preferred orientation for shear yielding introduced by Lazzeri and Bucknall [28] and Cheng *et al.* [29]. Lazzeri and Bucknall [28] proposed a theoretical model which predicts the formation of dilatational bands. According to this proposal, rubber-particle cavitation occurs in specific directions which results in the reduction of yield stress and, therefore, concentration of the shear deformation in those directions. The proposal of Cheng *et al.* [29] is based on observation of cooperative cavitation in rubber-toughened polycarbonate. These researchers explained the cooperative cavitation of nearby particles through impingement of plastic deformation at the equator of cavitated particles. The final result is the formation of cavitated arrays of particles, while the plastic deformation is concentrated within the arrays [29].

The existence of the connected structure in rubber-toughened epoxy, although possibly causing local variations in the direction of shear bands, does not change the overall shape of the crack tip plastic zone (Fig. 8). Therefore, the preferred orientation for shear yielding is not an issue in our discussion. The question, however, remains as to why the shear bands can further grow at the crack tip when the blend contains connected microstructure. Future research should address this issue plus the extent of the connectivity among the rubber particles in which the optimum mechanical properties are obtained.

4. Conclusion

Core–shell rubber particles with and without reactive groups in the shell polymer were included in two epoxy matrices. A variety of characterization techniques was employed. The following results were obtained.

1. The blend morphology in an epoxy modified by core–shell rubber particles was determined by firstly, the phase-separation mechanism of the shell material in the matrix and secondly, the kinetic competition between the phase separation and the curing reaction.

2. The immiscibility of PMMA in DGEBA epoxy after addition of the curing agent provides the driving force for aggregation of MBS particles which results in the formation of an inter-connected structure in the absence of reactive groups. Agitation of the blend prior to gelation suppresses clustering of MBS particles and results in more uniform dispersion of the rubbery phase.

3. The fracture toughness of a blend with a connected microstructure is significantly higher than that of a similar blend containing uniformly dispersed particles. The reason lies in the fact that the connected morphology enables shear bands to grow further at the crack tip. Therefore, the enlargement of the crack tip plastic zone is the reason for superiority of the connected microstructure.

4. Formation of the connected morphology also makes shear yielding easier in uniaxial tensile testing which results in reduced yield stress of the blend.

Although the results of this study illustrate the superiority of a connected morphology in improving the fracture toughness in rubber-modified epoxies, it does not specify the extent of the connectivity in which the optimum mechanical properties are obtained. Nor does it provide the rationale for further growth of shear bands when the rubber particles possess a connected microstructure. Therefore, future studies should investigate the optimum blend morphology in a more systematic fashion. Also, the micro-deformation mechanisms should be studied at a finer scale in blends with different morphologies.

Acknowledgements

The authors wish to acknowledge the financial support provided by Polymer Interfaces Center of Lehigh University and National Science Foundation (Grants MSS-9211664 and ECD-9117064).

References

1. C. B. BUCKNALL, "Toughened Plastics" (Applied Science, London, 1977).
2. J. N. SULTAN, R. C. LIABLE and F. J. McGARRY, *Polym. Symp.* **16** (1971) 127.
3. A. C. GARG and Y. W. MAI, *Compos. Sci. Technol.* **31** (1988) 179.
4. R. A. PEARSON and A. F. YEE, *J. Mater. Sci.* **26** (1991) 3828.
5. V. V. KOZII and B. A. ROZENBERG, *Polym. Sci.* **34** (1992) 919.
6. R. J. M. BORGGREVE and R. J. GAYMANS, *Polymer* **29** (1988) 1441.
7. E. A. FLEXMAN, D. D. HUANG and H. L. SNYDER, in "Polymer Preprints **29**, edited by C. K. Riew and A. J. Kinloch (ACS, Washington, 1988) p. 189.
8. K. YAMANAKA, Y. TAKAGI and T. INOUE, *Polymer* **30** (1989) 1839.
9. H. S. Y. HSICH, *Polym. Eng. Sci.* **30** (1990) 493.
10. H. J. SUE, E. I. GARCIA-MEITIN, D. M. PICKELMAN and P. C. YANG, in "Toughened Plastics", Advances in Chemistry Series, Vol. 233, edited by C. K.. Riew and A. J. Kinloch (ACS, Washington, 1993) p. 259.
11. K. YAMANAKA and T. INOUE, *Polymer* **30** (1989) 662.
12. B. G. MIN, J. H. HODGKIN and Z. H. STACHURSKI, *J. Appl. Polym. Sci.* **50** (1993) 1065.
13. A. MUKRAMI, D. SAUNDERS, K. OOISHI and T. YOSHIKI, *J. Adhes.* **39** (1992) 227.
14. T. IIJIMA, S. MIURA, W. FUKUDA and M. TOMOI, *Eur. Polym. J.* **29** (1993) 1103.
15. P. A. MATAGA, *Acta Metall.* **37** (1989) 3349.
16. Y. HUANG and A. J. KINLOCH, *J. Mater. Sci. Lett.* **11** (1992) 484.

17. R. A. PEARSON and A. F. YEE, *J. Mater. Sci.* **24** (1989) 2571.
18. R. BAGHERI, PhD dissertation, Lehigh University, Bethlehem, PA (1995).
19. H. J. SUE, R. A. PEARSON, D. S. PARKER, J. HUANG and A. F. YEE, *ACS Div. Polym. Chem. Polym. Prep.* **29** (1988) 147.
20. Rohm and Haas scientists, private communication (1993).
21. C. M. GOMEZ and C. B. BUCKNALL, *Polymer* **34** (1993) 2111.
22. S. REICH, *Phys. Lett.* **114A** (1986) 90.
23. M. CARPINETI and M. GIGLIO, *Phys. Rev. Lett.* **68** (1992) 3327.
24. D. J. ROBINSON and J. C. EARNSHAW, *ibid.* **71** (1993) 715.
25. I. C. HUANG, PhD dissertation, University of Michigan, Ann Arbor, MI (1994).
26. G. R. IRWIN, Appl. Mater. Res. **3** (1964) 65.
27. S. WU, *Polym. Eng. Sci.* **30** (1990) 753.
28. A. LAZZERI and C. B. BUCKNALL, *J. Mater. Sci.* **28** (1993) 6799.
29. C. CHENG, A. HILTNER, E. BAER, P. R. SOSKEY and S. G. MYLONAKIS, *ibid.* **30** (1995) 587.

Received 20 September 1995
and accepted 15 January 1996.